Multispectral Image-Based Binary Classification of Avocado Leaves' Vegetative Health Using Vegetation Indices and Convolutional Neural Networks

Kevin B. Carbajal[1][0009-0008-2510-040X], Alma Y. Alanis[1][0000-0001-9600-779X], Hamilton Oliveira[2][0000-0002-9590-7929], and Jorge Galvez[1][0000-0001-6595-8605]

[1] Universidad de Guadalajara, Guadalajara, México
kevin.bcs@hotmail.com, alma.alanis@academicos.udg.mx,
jorge.galvez@academicos.udg.mx
[2] Universidad Federal de Viçosa, Minas Gerais, Brasil
ogholiveira@gmail.com

Abstract. Avocado crops face challenges in detecting nutritional deficiencies that impact yield. This study proposes a binary classification of avocado leaves using multispectral imaging and convolutional neural networks (CNNs). Leaves are classified as healthy or affected based on visible symptoms. The dataset consists of 81 multispectral images (Green, Red, Red Edge, NIR) acquired with a DJI Mavic 3 Enterprise drone. Five vegetation indices (NDVI, GNDVI, NDRE, OSAVI, SAVI) and their statistical features were extracted to enhance learning. Data augmentation and dropout reduced overfitting. The CNN achieved 100% validation accuracy, and a comparative analysis of activation functions identified the best performers. Results demonstrate the potential of multispectral imaging and CNNs in precision agriculture. Future work will expand the dataset and spectral bands to improve detection.
Keywords: Convolutional Neural Networks · Multispectral Imaging · Vegetation Indices · Nutritional Deficiencies.

1 Introduction

Hass avocado (*Persea americana*, Hass variety) is one of Mexico's main export products, playing a crucial role in the national economy and international trade. The state of Michoacán, as the primary producing region, positions Mexico as the world's leading exporter of this fruit, making its study and monitoring essential to ensure its quality and sustainability [1]. However, avocado production faces challenges due to nutritional deficiencies that can impact yield if not detected in time.

[1] DJI Mavic 3 Enterprise Multispectral® is a registered trademark of DJI Technology Co., Ltd.

https://doi.org/10.61728/AE20255145

Recent advances in precision agriculture technologies have significantly improved the monitoring of crop vegetative health. The integration of sensors, meteorological stations, and satellite imagery has enhanced agricultural analysis. However, multispectral drones have proven to be particularly effective in the early detection of nutritional deficiencies [7].

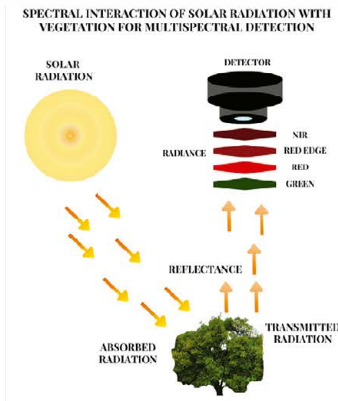

Fig. 1: Solar radiation strikes vegetation, where part of the energy is absorbed, another portion is transmitted through the leaves, and a fraction is reflected. The multispectral sensor captures the reflected radiation in different spectral bands, allowing the characterization of the vegetation's physiological state.

These sensors capture spectral information at different wavelengths, enabling the assessment of photosynthetic activity and the physiological state of the crop through vegetation indices such as the Normalized Difference Vegetation Index (NDVI), Green Normalized Difference Vegetation Index (GNDVI), Normalized Difference Red Edge Index (NDRE), Optimized Soil-Adjusted Vegetation Index (OSAVI), and Soil-Adjusted Vegetation Index (SAVI), which are widely used for detecting plant stress [6].

The cellular structure of leaves significantly influences the way they reflect electromagnetic radiation [7]. The **palisade mesophyll** is the primary photosynthetic region of the leaf, efficiently absorbing light in the blue (0.43 µm) and red (0.66 µm) bands, while the green band (0.54 µm) is more strongly reflected, giving the leaf its characteristic color [7].

The **spongy mesophyll**, with its intercellular spaces, internally scatters light, a notable effect in the NIR (0.7 – 1.2 µm), where reflectance increases due to the air-cell interaction within the leaf tissue [7]. Understanding this spectral interaction is essential for the accurate interpretation of multispectral images and the evaluation of crop physiological status.

Nutritional deficiencies in avocado crops have been identified through the visual analysis of specific symptoms on the leaves. These deficiencies affect the plant's physiology and can be detected based on their impact on leaf reflectance across different spectral bands [8].

- **Nitrogen (N)**: Its deficiency causes uniform chlorosis in older leaves due to reduced chlorophyll synthesis [8]. It can be detected using indices such as NDVI and GNDVI, which reflect light absorption in the R band [6].
- **Potassium (K)**: It manifests as necrosis on the leaf edges with a chlorotic halo around the affected area [8]. Changes in reflectance in the RE and NIR bands can indicate the presence of this deficiency [6].
- **Phosphorus (P)**: It appears as brown or purple spots on the leaves [8], with alterations in NIR reflectance, reflecting changes in water and protein content [6].
- **Calcium (Ca)**: In young leaves, its deficiency causes necrosis at the tips and deformations [8]. Its detection is based on decreased reflectance in the G and NIR spectrum [6].

(a) (b) (c) (d)

Fig. 2: Comparison of avocado leaves with different levels of nutritional deficiencies: (a) no symptoms, (b) mild, (c) moderate, and (d) severe.

2 Related Work

The use of multispectral imagery for detecting nutritional deficiencies in crops has been widely studied, demonstrating the effectiveness of vegetation indices in identifying physiological issues in plants and enabling early detection of nutritional deficiencies [2, 3].

Previous studies have applied various machine learning and CNN-based approaches for crop analysis. For example, in [3], a CNN was used to classify avocado leaves affected by thrips, demonstrating the effectiveness of deep learning in identifying foliar diseases. Other recent and highly relevant studies have employed neural networks to detect deficiencies and predict nitrogen ($\boldsymbol{N}$) percentages in gulupa leaves, using multispectral images combined with segmentation techniques to enhance model accuracy, yielding very promising results [2].

Drones equipped with multispectral cameras have been widely used in precision agriculture due to their ability to capture high-resolution images across multiple spectral bands [4, 7]. Their use, in combination with artificial intelligence techniques, has shown promising results in the automatic detection of crop anomalies. While there are studies on the use of CNNs and vegetation indices in agriculture, their specific application in the classification of avocado leaves still requires further research.

Methodology

This study proposes a methodology for the binary classification of avocado leaves using multispectral imaging and deep learning, leveraging the effectiveness of convolutional neural networks (CNNs) in agricultural pattern recognition [2]. Unlike previous research, this approach integrates five vegetation indices (NDVI, GNDVI, NDRE, OSAVI, and SAVI) as inputs for a CNN, optimizing the detection of nutritional deficiencies. T he f usion o f m ultispectral d ata w ith artificial intelligence enhances classification a ccuracy, e nabling m ore i nformed decision-making in precision agriculture [2, 6].

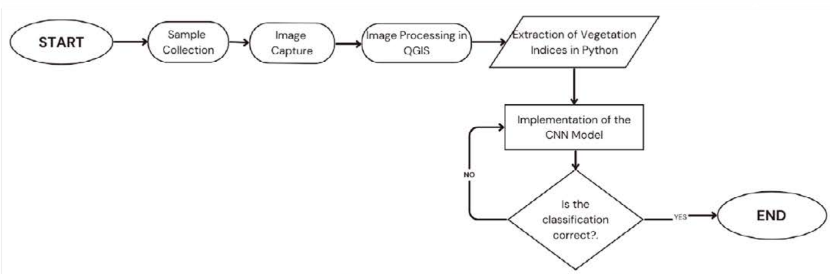

Fig. 3: Flowchart of the methodology used in this study.

The research was conducted at two institutions: (1) the Association of Producers and Packers of Avocados of Mexico (APEAM), where sample collection, visual classification of leaves, and multispectral image acquisition were performed, and (2) the Center for Exact Sciences and Engineering of the University of Guadalajara (CUCEI), where image processing, data analysis, and the development of the CNN model were carried out.

3.1 Leaf Collection

Hass avocado leaf samples were collected from an orchard located in Salvador Escalante, Michoacán, bordering Cuitzitán and Santa Clara del Cobre. The orchard spans 43 hectares. The leaf collection was conducted in collaboration with an agronomist specializing in avocado orchards, who assessed symptoms associated with nutritional deficiencies and visible diseases in the leaves, focusing on deficiencies of N, P, K, Ca, B, and Zn [8].

The collected leaves were transported to the Asociación de Productores y Empacadores Exportadores de Aguacate de México (APEAM), where a secondary classification was performed based on identified deficiencies. A total of 134 leaves were photographed for analysis and labeled into two categories: (1) healthy leaves, showing no visible deficiency symptoms, and (2) affected leaves, exhibiting signs of nutritional stress.

3.2 Multispectral Image Acquisition

The capture of multispectral images was conducted using the DJI Mavic 3M drone, which is equipped with a multispectral camera equipped with four 5-megapixel sensors, designed to capture information in the following bands:

- **G**: 560 nm ± 16 nm
- **R**: 650 nm ± 16 nm
- **RE**: 730 nm ± 16 nm
- **NIR**: 860 nm ± 26 nm

Thanks to these features, the DJI Mavic 3M is a high-precision tool for smart farming, enabling detailed crop development monitoring and early detection of nutritional deficiencies [4].

To capture the images, a custom mount was implemented to achieve the necessary height for the camera to focus on the leaves. Additionally, a black background was used to prevent shadows or noise in the reflectance. The photographs were taken using sunlight as the reflectance source.

Fig. 4: DJI Mavic 3M drone used for multispectral image capture.

3.3 Initial Image Processing in Quantum Geographic Information System (QGIS)

The captured images were processed in QGIS, where georeferencing was applied to align them with geographic coordinates, spectral calibration was performed to correct distortions, and raster segmentation was used to isolate avocado leaves, removing noise. Finally, the four multispectral bands (G, R, RE, NIR) were combined for each leaf, generating a complete spectral representation for analysis.

[2] QGIS® is a registered trademark of the QGIS Development Team.
[3] Python® is a registered trademark of the Python Software Foundation.
[4] OpenCV® is a registered trademark of OpenCV.org.

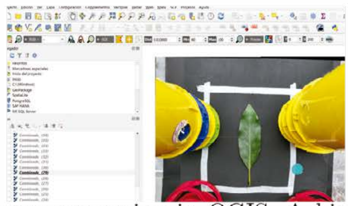

Fig. 5: Multispectral image processing in QGIS. A higher resolution image is available at the link in the supplementary material section.

3.4 Dataset and Data Augmentation

To enhance the model's generalization capability and compensate for the limited size of the original dataset, various strategies were implemented to expand the available information for deep learning, including data augmentation, which is explained later in the text. It is important to highlight that although the initial dataset consists of 81 multispectral images, each image is composed of four spectral bands (G, R, RE, and NIR) resulting in a total of 324 individual spectral representations. Additionally, statistical data extraction from five vegetation indices was performed.

3.5 Image Processing and Vegetation Index Extraction

Image processing was performed in Python using Rasterio and OpenCV for raster data manipulation. From the multispectral images, five vegetation indices were computed to assess photosynthesis, chlorophyll content, and cellular structure, providing an accurate estimation of vegetative health.

- **NDVI**: Uses the NIR and R bands. It is calculated using the following formula:

$$NDVI = \frac{NIR - R}{NIR + R} \tag{1}$$

  This index is used to assess biomass and photosynthetic activity in leaves. In this study, healthy leaves are expected to have higher NDVI values due to greater absorption in the red band and higher reflectance in the NIR band [6].

- **GNDVI**: Uses the NIR and G bands. Its formula is:

$$GNDVI = \frac{NIR - G}{NIR + G} \tag{2}$$

  This index is more sensitive to chlorophyll concentration in leaves compared to NDVI. In healthy leaves, a high GNDVI value is expected, indicating a high photosynthetic capacity. In leaves with ***N, P***, or ***K*** deficiencies, GNDVI values are likely to decrease due to reduced chlorophyll production and the onset of chlorosis [6].

- **NDRE**: Uses the NIR and RE bands. It is expressed as:

$$NDRE = \frac{NIR - RE}{NIR + RE} \quad (3)$$

NDRE is particularly useful for detecting early-stage stress, as the RE band is more influenced by the internal cellular structure of leaves. In leaves with visible symptoms of $\boldsymbol{Ca}$ and $\boldsymbol{Zn}$ deficiencies, NDRE tends to be lower due to cellular damage and reduced nutrient transport efficiency [6].

- **OSAVI**: This index adjusts for soil influence in vegetation measurements. It is defined as:

$$OSAVI = \frac{(NIR - R)}{(NIR + R + 0.16)} \quad (4)$$

Unlike NDVI, OSAVI corrects for soil effects, making it useful in conditions where vegetation is not dense [6].

- **SAVI**: The SAVI index is a variation of NDVI that incorporates a soil correction factor L, which is useful in areas with intermediate vegetation cover ($L = 0.5$). Its equation is:

$$SAVI = \frac{(NIR - R)}{(NIR + R + L)}(1 + L) \quad (5)$$

In this study, it is used to assess leaf hydration. Low values indicate water stress or severe nutritional deficiencies due to reduced water absorption and alterations in NIR reflectance [6].

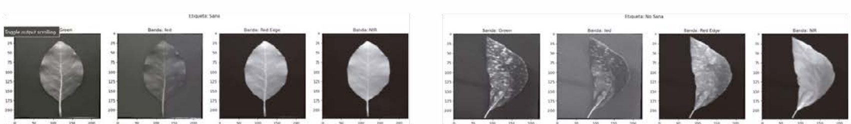

(a) (b)

Fig. 6: Comparison of multispectral images in the four spectral bands. (a) Avocado leaves with no visible symptoms of nutritional deficiencies. (b) Avocado leaves showing visible symptoms of nutritional deficiencies. High-resolution images are available in the supplementary material section.

4 Statistical Analysis of Vegetation Indices

The statistical data for the five vegetation indices used in the analysis of avocado leaves are presented below. The data include the mean, minimum, maximum, variance, and standard deviation. [5]

[5] Statistical data can be accessed at: `https://drive.google.com/drive/folders/1yIAxyrnHt-nRh2wXdKnbwYnnw8zgwRof?usp=sharing`.

Table 1: Statistical Data of NDVI

Leaf	Mean	Minimum	Maximum	Variance	Std. Dev.
No Symptoms 1	-0.2405	-0.9999	0.4231	0.1005	0.3171
No Symptoms 2	-0.2232	-0.9999	0.5338	0.0952	0.3085
With Symptoms 1	-0.3026	-0.6551	0.4127	0.1014	0.3185
With Symptoms 2	-0.2739	-0.5631	0.4457	0.1104	0.3322

Healthy leaves exhibit higher NDVI values (-0.14 to -0.33), whereas those with symptoms show lower NDVI values (-0.28 to -0.38), indicating lower light absorption in the red band and reduced photosynthetic efficiency.

Table 2: Statistical Data of GNDVI

Leaf	Mean	Minimum	Maximum	Variance	Std. Dev.
No Symptoms 1	-0.2037	-0.9999	0.3651	0.0566	0.2378
No Symptoms 2	-0.2277	-0.9999	0.3951	0.0533	0.2308
With Symptoms 1	-0.1569	-0.7199	0.4498	0.0568	0.2384
With Symptoms 2	-0.1757	-0.6572	0.5999	0.0719	0.2681

GNDVI shows that unhealthy leaves exhibit greater chlorophyll variability and lower light absorption in the green band, indicating physiological stress. Its usefulness lies in the early detection of nutritional deficiencies, as the damage is progressive and non-uniform.

Table 3: Statistical Data of NDRE

Leaf	Mean	Minimum	Maximum	Variance	Std. Dev.
No Symptoms 1	-0.0289	-0.3801	0.9999	0.0053	0.0726
No Symptoms 2	-0.0368	-0.3203	0.9999	0.0056	0.0746
With Symptoms 1	-0.0127	-0.5855	0.3884	0.0050	0.0707
With Symptoms 2	-0.0309	-0.3427	0.4221	0.0053	0.0725

NDRE shows that unhealthy leaves exhibit greater variability in red edge light absorption, indicating early structural changes in the leaf. Its variability makes it useful for detecting stress before symptoms become visible.

Table 4: Statistical Data of OSAVI

Leaf	Mean	Minimum	Maximum	Variance	Std. Dev.
No Symptoms 1	-0.1648	-0.8581	0.3588	0.0606	0.2461
No Symptoms 2	-0.1534	-0.8576	0.4726	0.0592	0.2434
With Symptoms 1	-0.2266	-0.5575	0.3652	0.0644	0.2537
With Symptoms 2	-0.1941	-0.4618	0.3895	0.0677	0.2601

OSAVI shows that unhealthy leaves exhibit lower values compared to healthy ones, indicating reduced reflectance in the NIR band.

Table 5: Statistical Data of SAVI

Leaf	Mean	Minimum	Maximum	Variance	Std. Dev.
No Symptoms 1	-0.1437	-0.9889	0.4067	0.0657	0.2562
No Symptoms 2	-0.1334	-0.9877	0.5699	0.0668	0.2584
With Symptoms 1	-0.2202	-0.6351	0.4412	0.0722	0.2687
With Symptoms 2	-0.1763	-0.5011	0.4608	0.0737	0.2715

SAVI indicates that unhealthy leaves have more negative values compared to healthy ones, suggesting lower water content and structural alterations in the leaf. Their lower reflectance in the NIR band confirms the presence of physiological stress.

5 CNN Architecture

5.1 Environment Setup and Libraries

For the development of the model, numerical processing and multispectral image manipulation libraries were used, such as `NumPy`, `rasterio`, `OpenCV`, and `TensorFlow`. The core code was implemented in `Python`, using `Keras` for building the CNN.

5.2 Calculation and Analysis of Vegetation Indices

From the multispectral images, five vegetation indices were calculated. Additionally, their statistical features were extracted to enrich the dataset and improve classification in the CNN.

5.3 Image Preprocessing

The multispectral images in `.tif` format were processed using `rasterio` and resized to 224×224 pixels for use in the CNN. The preprocessing steps included calculating vegetation indices, extracting statistical features, and labeling the images as either 'leaf without symptoms' or 'leaf with symptoms'.

5.4 Feature Vector Construction

A feature vector was created by combining the normalized multispectral image ($224 \times 224 \times 4$) with a set of 25 statistical features from the vegetation indices. This combination allows the CNN to leverage both spatial information and numerical metrics, enhancing classification accuracy.

5.5 Data Loading and Concatenation

The images and labels from both groups were loaded and concatenated into a single data matrix, along with the statistical features of the vegetation indices.

5.6 Dataset Splitting

To ensure proper generalization of the model, the dataset was divided into two subsets:

- **Training (80%):** Used to adjust the model's weights during the learning process.
- **Testing (20%):** Used to evaluate the model's performance on unseen data and assess potential overfitting issues.

The partitioning was performed using the `train_test_split()` function from *Scikit-learn*, setting the `random_state` parameter to 42 to ensure experiment reproducibility.

6 CNN Model Design

6.1 Dual-Input Model

To improve the classification of avocado leaves, a CNN model with a dual-input architecture was designed. This approach allows the combination of visual information from multispectral images with numerical statistics from vegetation indices, providing a more comprehensive representation of each sample.

6.2 Image Processing Pathway

The model processes multispectral images of size $224 \times 224 \times 4$ (corresponding to the G, R, RE, and NIR bands) through three convolutional layers with 3×3 filters, each followed by a non-linear activation function and a *MaxPooling* layer to reduce dimensionality. Several activation functions were tested, including *LeakyReLU*, *ReLU*, *Sigmoid*, *Tanh*, *ELU*, *SELU*, *Softplus*, *Softsign*, *Swish*, and *GELU*, to evaluate their effectiveness in classification.

6.3 Statistics Pathway

A second input channel processes a vector containing 25 features extracted from the NDVI, GNDVI, NDRE, OSAVI, and SAVI indices. This vector is processed through a fully connected layer with 64 neurons, using the activation function selected in each experiment.

6.4 Fusion and Classification

Both pathways are combined through a concatenation layer, followed by a dense layer with 128 neurons and a non-linear activation function. A *Dropout* layer with a 50% rate was applied to reduce overfitting. Finally, a single neuron with a sigmoid activation function generates the binary classification prediction (healthy or affected leaf).

6.5 Compilation and Optimization

The model was compiled using the *binary cross-entropy* loss function and the *Adam* optimizer with a learning rate of 0.0001. The performance of each activation function were compared in terms of accuracy, loss, and training time.

6.6 Model Training and Configuration

The CNN model was trained using a dataset that combines multispectral images ($224 \times 224 \times 4$) and a statistical feature vector containing 25 characteristics extracted from vegetation indices.

To enhance the model's generalization ability and reduce overfitting, *data augmentation* was applied using `ImageDataGenerator`. The applied transformations included:

- Random rotation of up to 20°.
- Horizontal and vertical shifts of up to 20%.
- Shear transformations.
- Random zoom of up to 20%.
- Horizontal image flipping.

Training was performed with a batch size of 8, the *Adam* optimizer ($lr = 0.0001$), and the *binary cross-entropy* loss function, for a total of 100 epochs.

6.7 Evaluated Activation Functions

To optimize the model's performance, various activation functions were tested in the convolutional layers. The comparative results in terms of accuracy, loss, and training time are presented in Table 6.

Activation Function	Accuracy (%)	Loss	Time (s)
LeakyReLU	94.12	0.2028	190.40
ReLU	100.00	0.0484	188.05
Sigmoid	35.29	0.7014	191.15
Tanh	100.00	0.0553	191.85
ELU	100.00	0.1215	195.92
SELU	100.00	0.0391	195.88
Softplus	35.29	0.6948	213.70
Softsign	100.00	0.0890	192.22
Swish	94.12	0.1351	228.14
GELU	100.00	0.0507	250.25

Table 6: Comparative results of activation functions.

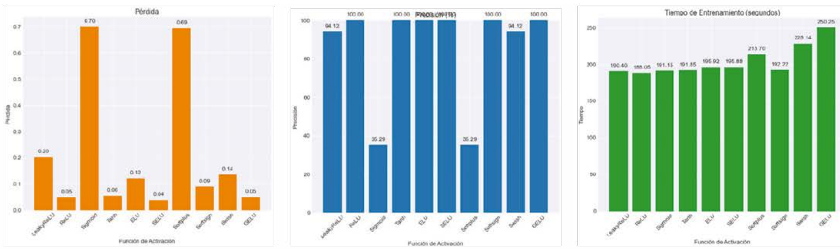

(a) (b) (c)

Fig. 7: Comparison of activation functions based on (a) loss , (b) accuracy , and (c) training time (seconds). High-resolution images are available in the supplementary material section.

[3]

As observed in Table 6, the ReLU, Tanh, SELU, Softsign, and GELU functions achieved high accuracy after 100 epochs, with variations in loss and training time. SELU performs well with low loss, while ReLU is one of the fastest and most effective activation functions.

Functions such as Sigmoid and Softplus are not suitable for this problem due to their low accuracies and high losses.

GELU provides a good balance between accuracy and loss; however, its high training time makes it less efficient for time-sensitive tasks.

7 Results and Analysis

7.1 Model Evaluation and Metrics

The model's performance was evaluated on the test set (20% of the data) to assess its generalization capability on unseen data. Metrics such as accuracy and loss were computed for both training and validation, along with the confusion matrix to identify false positives and false negatives. These metrics were used to monitor learning stability and detect potential overfitting issues. The obtained metrics were as follows:

[3] For better visualization, high-resolution images are available at: `https://drive.google.com/drive/folders/1yIAxyrnHt-nRh2wXdKnbwYnnw8zgwRof?usp=sharing`.

Leaf Type	Precision	Recall	F1-score
No Symptoms (0)	1.00	1.00	1.00
With Symptoms (1)	1.00	1.00	1.00

Table 7: Classification metrics of the CNN model.

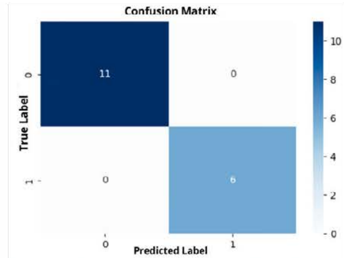

Fig. 8: Confusion matrix of the CNN model.

The CNN model achieved perfect classification, with 100% accuracy, recall, and F1-score. The confusion matrix indicates zero errors, correctly classifying all leaves with and without symptoms.

The accuracy and loss curves during training are presented in Figure 9:

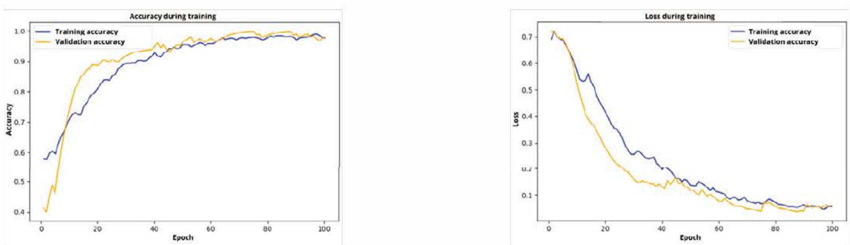

(a) (b)

Fig. 9: Evolution of accuracy and loss during CNN model training. (a) Accuracy during training and validation, showing a progressive improvement in model performance. (b) Loss during training and validation, illustrating a gradual decrease in error. Both metrics stabilize over time, indicating that the model has reached optimal convergence without significant overfitting. High-resolution images are available in the supplementary material section.

8 Discussion

The obtained results demonstrate the effectiveness of the dual-input CNN model in classifying avocado leaves with and without symptoms of nutritional deficiencies. The combination of multispectral images and statistical vegetation index data improved the model's accuracy, achieving 100% accuracy on the test set.

The activation function analysis showed that *ReLU*, *SELU*, and *GELU* achieved better performance in terms of accuracy and loss, while *Sigmoid* and *Softplus* exhibited lower performance. Additionally, the NDVI and GNDVI indices revealed reduced photosynthetic activity in affected leaves, validating their usefulness in detecting nutritional stress.

The use of *data augmentation* helped prevent overfitting and improve the model's generalization, although some activation functions increased training time.

Despite the positive results, the dataset size remains a limitation. Although 324 multispectral images were processed, the combination of the four bands reduced the final dataset to only 81 images for training. Expanding the dataset and implementing a multiclass classification approach would enhance the model's capability, allowing for a more precise differentiation of foliar conditions. Additionally, incorporating nutrient concentration prediction, utilizing more spectral bands, and evaluating more advanced models could further optimize the system's accuracy.

9 Conclusion

This study confirms that combining multispectral images and statistical vegetation index data in a dual-input CNN model is an effective strategy for classifying avocado leaves based on their physiological state.

The model achieved 100% accuracy, demonstrating its ability to identify symptoms of nutritional deficiencies in avocado crops. The choice of activation functions significantly influenced the model's performance, with $ReLU$, $SELU$, and $GELU$ being the most effective.

To further enhance the model's robustness, it is recommended to expand the dataset, explore the use of pre-trained neural networks, and consider self-supervised learning approaches. These advancements will improve the early detection of nutritional stress in crops, contributing to the development of precision agriculture.

Acknowledgments

Special thanks to Ing. Samuel Carbajal Mercado, the Association of Producers and Exporters of Avocado from Mexico, for their support during the research.

Supplementary Material

To facilitate access to the visual data used in this study, high-resolution images and statistical data can be found at the following link:

`https://drive.google.com/drive/folders/1yIAxyrnHt-nRh2wXdKnbwYnnw8zgwRof?usp=sharing`

This supplementary material includes expanded versions of the figures presented in the document, allowing for better visualization and analysis of relevant details.

References

1. FAO-FAOSTAT. "La exportación de aguacate en el mundo," ProducePay, 2020. Disponible en: `https://www.fao.org/faostat/es/#data/QCL`. Accedido: 13-sep-2024.
2. Gómez, J., Rincón, J., Quintero, H.: *Desarrollo de una herramienta de aprendizaje automático que estime el estado de N presente en las hojas de gulupa usando imágenes multiespectrales*. Universidad Nacional de Colombia (2021).
3. Huamán-Ampuero, J.: *Data Set de Imágenes de Hojas de Palta Para Detección de Enfermedad Causadas por Trips*. Revista de Investigación MICAELA, vol. 5, no. 1, pp. 36-41 (2024). Disponible en: `https://www.researchgate.net/publication/385092774_Data_Set_de_Imagenes_de_Hojas_de_Palta_Para_Deteccion_de_Enfermedad_Causadas_por_TripsDataset_of_Avocado_Leaf_Images_for_Detection_of_Disease_Caused_by_Thrips`.
4. DJI: *DJI Mavic 3M - Especificaciones técnicas*. DJI Enterprise. Disponible en: `https://ag.dji.com/es/mavic-3-m` (2023).
5. Zavala-Segoviano, A., Cabrera-Sixto, J.M.: *Identificación de las deficiencias de N, P y K en maíz (Zea mays) mediante técnicas de percepción remota*. Congreso Internacional de Investigación e Innovación 2016, pp. 1-6 (2016). Disponible en: `https://congresoucec.com.mx/documentos/mem2016/Ponencias/P-UCEC383.pdf`
6. Sergieieva, K.: *Índices de vegetación y teledetección en agricultura de precisión*. EOS Data Analytics, EOS Blog (2023). Disponible en: `https://eos.com/es/blog/indices-de-vegetacion/`. Publicado el 18-feb-2022.
7. Jensen, J.R.: Remote Sensing of the Environment: An Earth Resource Perspective. 2nd edn. Pearson Prentice Hall, Upper Saddle River (2007)
8. Park, C.H., Gaona, P., Viteri Díaz, P., Merino Toro, J., Viera Arroyo, W., Mejía Bonilla, P., Hinojosa Acurio, M., Noboa Basantes, M.: *Revisión bibliográfica de las deficiencias de nutrientes en aguacate*. KOPIA - INIAP, Ecuador (2023).